RSC Advances

ROYAL SOCIETY OF CHEMISTRY

www.rsc.org/advances

Simultaneous ultrasonic-assisted removal of malachite green and safranin O by copper nanowires loaded on activated carbon: central composite design optimization

Mostafa Roosta*, Mehrorang Ghaedi, Arash Asfaram

Chemistry Department, Yasouj University, Yasouj 75918-74831, Iran

Abstract

The present study investigates the simultaneous ultrasound-assisted adsorption of malachite green (MG) and safranin O (SO) dyes from aqueous solutions by ultrasound-assisted adsorption onto copper nanowires loaded on activated carbon (Cu-NWs-AC). In this study a novel and green approach described for the synthesis of Cu nanowires. This novel material was characterized using different techniques such as FESEM, XRD, EDS and UV-Vis. The effects of variables such as sonication time, pH, adsorbent dosage and initial dyes concentrations on the simultaneous dyes removal were studied and optimized by a central composite design (CCD) combined with desirability function (DF). A good agreement between experimental and predicted data using optimal model in this study was observed. These results indicate that a small amount of proposed adsorbent (0.022 g) was applied for simultaneous removal of 15 mg L^{-1} of malachite green and 15 mg L^{-1} of safranin O (>99%) in a short time (6.0 min) and pH of 5.5.

Keywords: Activated carbon; Adsorption; Central composite design; Copper nanowires;

* Corresponding author. Tel.: +98 741 2223048; fax: +98 741 2223048
E-mail: mostafaroosta.mr@gmail.com

1. Introduction

Dyes extensively used in textile, dyeing, electroplating, printing, tanneries and related industries and their discharge into wastewater generate contaminated environment. [1-3] Therefore, the dyes removal from industrial effluents are challenging requirement and help to produce safe and clean media. MG consume in silk, wool, cotton, leather and paper (Fig. 1a) also employed as therapeutic agent to treat parasites, fungal and bacterial infections.[4, 5] SO (Fig. 1b) is used as biological stain, histology, cytology and detection of cartilage and mast cell granules. [6] Extensive usage of adsorption for wastewater treatment is related to properties such as high efficiency, capacity and large scale ability of re-generable adsorbents.[7-10] Nanometer adsorbent with special physical and chemical properties (presence of various surface reactive sites and high surface to volume ratio) attain much focus and applicability in adsorption and separation sciences.[11-14] Activated carbon (AC) due to distinguished remarks viz. low cost and porous structure are good and re-usable support for loading nanomaterial that simultaneously lead to increase in number and type of reactive centers and increase life time of adsorbents , while simultaneously reduce its toxicity and facilated phase separation. [4, 15-17] Synthesized and characterized Cu-NWs-AC was applied for the simultaneous removal of MG and SO, while adsorption rate was accelerated via ultrasonic power and determination of non-adsorbed dyes simply and cost-effective manner was done by UV-Vis detection.

Sonochemistry has received considerable interest over the past few decades due to its ability as acoustic cavitation divided to formation, growth and collapse of micrometrical bubbles emerged from propagation of a pressure wave through a liquid. Ultrasound has been proven to be a very useful tool in enhancement of rate of mass transfer in sorption process and increased/facilitated pore diffusion and breaking the affinity between adsorbate and adsorbent.[18-20] Combination of ultrasound with adsorption process was found to be more promising in the

removal of pollutants like dyes and metal ions.[21-24] The use of ultrasound in degradation of dyes has reported in recent decades.[25-28] Ultrasound events such as micro-streaming, micro-turbulence, acoustic (or shock) waves and microjets possible enhance in performance of adsorption/desorption system.[19, 27, 29-32] Shock waves have the potential of creating microscopic turbulence within interfacial films surrounding nearby solid particles. Acoustic streaming induced by the sonic wave is the movement of the liquid, which means conversion of sound to the kinetic energy.

Designing and optimization of experiments and evaluation of the variables influence is better to achieve in simultaneous optimization to estimate the presence and magnitude of their interaction. Statistical design of experiment possible such purpose by at least number of experiments.[33, 34] Response surface methodology (RSM) is good and appropriate tool for designing experiment, constructing models, evaluating the effects of multiple factors and investigating optimum conditions.[35] RSM combined with CCD and DF possible to investigate full detail of influence of variables such as sonication time, pH, initial MG and SO concentrations and adsorbent dosage.

2. Experimental

2.1. Instruments and Reagents

An ultrasonic bath with heating system (Tecno-GAZ SPA Ultra Sonic System, Bologna, Italy) at 40 KHz of frequency and 130 W of power was used for the ultrasound-assisted adsorption procedure. The pH measurements were carried out using a digital pH meter (Ino Lab pH 730, Germany) and the dyes concentrations were determined using Jasco UV-Vis spectrophotometer model V-530 (Jasco, Japan) at a wavelength of 619 and 521 nm respectively for MG and SO.

The atomic composition of the Cu-NWs-AC was analyzed by energy-dispersive X-ray spectrometer (EDX) using an Oxford INCA II energy solid state detector. X-ray diffraction (XRD) pattern was recorded by an automated Philips X'Pert X-ray diffractometer (Philips Analytical X-Ray, Netherlands) with Co Kα radiation (40 kV and 30 mA) for 2θ values over 10-100º. For XRD analyses, solid samples of the Cu NWs were separated from the aqueous suspension by centrifugation at 4000 rpm with dilute hydrazine solution and then nitrogen gas was gently blown into it to dry the sample. The shape and surface morphology of the Cu NWs were investigated by field emission scanning electron microscope (FE-SEM, Hitachi S4160, Tokyo, Japan) under an acceleration voltage of 15 kV.

Absorption measurements of nanoparticles were carried out on a Perkin Elmer Lambda 25 spectrophotometer (Massachusetts, USA) using a quartz cell with an optical path of 1 cm. The stock solutions (200 mg L^{-1}) of MG and/or SO were prepared by dissolving 20 mg of each solid dye in 100 mL double distilled water and the working concentrations daily were prepared by their suitable dilution. All chemicals including NaOH and HCl with the highest purity available were purchased from Merck (Darmstadt, Germany).

2.2. Ultrasound assisted adsorption method

The ultrasound assisted adsorption method was carried out in a batch mode as follows: 50 mL of 15 mg L^{-1} of MG and SO at pH of 5.5 was mixed with 0.022 g of Cu-NWs-AC that dispersed thoroughly following sonication time of 6.0 min at room temperature. At each stage, the sample was immediately centrifuged and analyzed by UV-Vis spectrophotometry at maximum wavelength over working concentration. The efficiency of dyes removal was determined at different experimental condition according CCD method. The dyes removal percentages were calculated using the following equation:

$$\% \text{ dye removal} = ((C_0 - C_t)/C0) \times 100 \quad (1)$$

where C_0 (mg L^{-1}) and C_t (mg L^{-1}) is the concentration of target at initial and after time t respectively.

2.3. Preparation of carbon-supported Cu nanowires (Cu-NWs-AC)

The Cu-NW was prepared as follow: 150 mL of NaOH solution (7 mol L^{-1}) and 7.5 mL of copper nitrate (0.1 mol L^{-1}; aqueous solution) were added to 250 mL glass reactor. Then, 1.95 mL of ethylenediamine (99%) and 0.75 mL of hydrazine solution (2.8 mol L^{-1}) added and mixed thoroughly. Holding this mixture in bath of 60 °C for 45 min cause that royal blue of solution changed to bronze after 38 min (formation of the Cu nanowires). 150 mL of the freshly prepared Cu NWs solution addition to activated carbon (30 g) in a 250 mL flask under magnetic stirring for up to 4 h lead to formation of Cu-NWs-AC and were generally dried at 110 °C for 12h. [36] A mortar was used to homogeneously grind carbon-supported Cu NWs powder. The Cu-NWs-AC was stored in air at room temperature.

2.4. Central composite design

The CCD (five-level with α value fixed at 2.0, rotatable) designed by using the STATISTICA 7) based on 32 runs was used to investigate the effects of sonication time, pH, amount of adsorbent, MG concentration and SO concentration (Table 1). The center points are used to determine the experimental error and the reproducibility of the data. Table 2 shows the experimental design points consists of 2^n factorial points with 2n axial points and Nc central points and the test results for the response variables. The independent variables are coded to the

(−1, +1) interval where the low and high levels are coded as −1 and +1, respectively. The axial points are located at distance of α from center and make the design rotatable.

The mathematical relationship between the five independent variables can be approximated by the second order polynomial model: [37, 38]

$$y = \beta_0 + \sum_{i=1}^{5} \beta_i x_i + \sum_{i=1}^{5} \sum_{j=1}^{5} \beta_{ij} x_i x_j + \sum_{i=1}^{5} \beta_{ii} x_i^2 \quad (2)$$

where y is the predicted response (removal percentage); X_i's are the independent variables (sonication time, pH, amount of adsorbent, MG concentration and SO concentration) that are known for each experimental run. The parameter β_0 is the model constant; β_i is the linear coefficient; β_{ii} are the quadratic coefficients and β_{ij} are the cross-product coefficients.

2.5. Desirability function

A desirability function (DF) is an established technique based on Derringer's desirability function. [39] Each predicted response $\hat{U}_i$ and experimental response U_i can be transformed to create a function for each individual response d_i and finally determine a global function D that should be maximized following selection of optimum value of affective variables with considering their interaction. Firstly, the response (U) is converted into a particular desirability function (df_i) in the range of 0 to 1. The d_i=0 represents completely undesirable response or minimum applicability and di=1 represents completely desirable or ideal response. The individual desirability scores d_is are then combined using geometrical mean, on a single overall (global) desirability D, which is optimized to find the optimum set of input variables:

$$DF = [df_1^{v1} \times df_2^{v2} \ldots \times df_n^{vn}]^{1/n}, 0 \leq vi \leq 1 \quad (i = 1, 2, \ldots, n) \qquad (3)$$

$$\sum_{i=1}^{n} vi = 1$$

where df_i indicate the desirability of the response Ui (i = 1, 2, 3,..., n) and vi represents the importance of responses.

The individual desirability function for the ith characteristic is computed via following equation that α and β are the lowest and highest obtained values of the response i and w_i is the weight:

$$df_i = \left(\frac{U-\alpha}{\beta-\alpha}\right)^{wi}, \alpha \leq U \leq \beta \qquad (4)$$

$$df_i = 1, \ U > \beta$$

$$df_i = 0, \ U < \alpha$$

3. Results and discussion

3.1. Characterization of adsorbent

Hydrazine act as reducing agent for transformation of Cu^{2+} ions into Cu^0 that the reaction were accelerated and catalyzed by large amount of NaOH aqueous solution. The extent of reaction was followed by visual and spectrophotometric study. The Cu NWs similar to other zero-vallent element indicate distinguish and sensitive absorption peak correspond to Surface Plasmon Resonance (SPR) [40] (Fig. 2 a). Peak has maximum at wavelength of about 575 nm and support the narrow size distribution of the Cu NWs and has good correlation with size of nano-structure so that shifts to the shorter wavelengths with decreasing size of the nanowires (quantum confinement). [36, 41]

X-ray diffraction (XRD) pattern of Cu NWs powder (Fig. 1(b)) has good agreement with standard copper XRD pattern (Joint Committee for Powder Diffraction Standards, JCPDS, NO. 65-9743; bottom of Fig. 2 b). It exhibit three major diffraction peaks related to the diffraction angles at around 44.16º, 51.60º, 73.81 º and 89.32º related to the planes (111), (200), (220) and (311) and proofed the face-centered cubic lattice structure of copper NWs.[42, 43] There was not found any diffraction peaks correspond to CuO or Cu_2O in the XRD pattern. The average nanocrystallites size (D) is estimated according to the Debye–Scherer Eq based on K of 0.9 and X-ray wavelength λ (1.78897 °A) belong to the most intense peak (111) was estimated to be about 75 nm:[44]

$$D = \frac{K\lambda}{\beta \cos\theta} \quad (5)$$

The FESEM images of the activated carbon surface and the Cu NWs deposited on activated carbon are shown in Fig. 3a and b. It can be seen that the surface morphology of the activated carbon are homogeneous and relatively smooth. Fig. 3b shows the detailed morphologies of the Cu NWs deposited on the activated carbon which are composed of a large quantity of well-dispersed Cu NWs. The average diameter of the Cu NWs is ~ 81 nm as calculated from 20 nanowires randomly selected from the SEM image. The lengths of the nanowires vary from tens to hundreds of micrometers

In order to further confirm the composition on the surface of copper nanowires loaded on activated carbon, the energy-dispersive spectra (EDS) from different sample spots were performed. The EDS spectra of Cu-NWs-AC and the quantitative elemental composition were shown in Fig. 4.

The EDS mapping of the Cu-NWs-AC was presented in Fig. 4(a) in order to investigate their localized elemental information. It is worth noting that the element of Cu was well dispersed on the surface of Cu-NWs-AC.

Fig. 4(a) and (b) confirmed the presence of C and Cu in Cu-NWs-AC. The C signal is originated from the activated carbon while the Cu signal came from the Cu-NWs nanoparticles, which confirms the existence of Cu-NWs, consistent with the results of XRD and SEM.

3.2. Central composite design (CCD)

CCD design and its further analysis (Tables 1 and 2) for following variables (sonication time (X_1), pH (X_2), adsorbent dosage (X_3), MG concentration (X_4) and SO concentration (X_5)) according to prescribed above conditions (32 experiments) were undertaken. To find the most important effects and interactions, analysis of variance (ANOVA) was calculated using STATISTICA 7.0 (Table 3). A p-value less than 0.05 in the ANOVA table indicates the statistical significance of an effect at 95% confidence level. F-test was used to estimate the statistical significance of all terms in the polynomial equation within 95% confidence interval. Data analysis gave a semi-empirical expression of removal percentage with following equation:

$$y = 71.93 + 11.79x_1 + 7.46x_2 + 15.69x_3 - 5.62x_4 - 4.60x_5 - 2.11x_1^2 - 2.96x_2^2 - 4.01x_3^2 - +2.99x_1x_4 - 8.07x_2x_3 + 2.78x_2x_5 - 3.05x_3x_4 \quad (6)$$

The plot of experimental values of removal (%) values versus those calculated from equation indicated a good fit, as presented in Fig. 5.

3.3. Response surface methodology

Response surface methodology (RSM) was developed by considering all the significant interactions in the CCD to optimize the critical factors and describe the nature of the response surface in the experiment. Fig. 6 represents the most relevant fitted response surfaces for the design and depicts the response surface plots of removal (%) versus significant variables and their curvatures support the presence of interaction among the variables.

The effect of initial MG concentration on its removal percentage and the interaction of it by some factors were shown in Fig. 6 (a, d). It was seen that in despite of the increase in the amount of dye uptake, its removal efficiency was decreased and at lower dye concentrations, the ratio of solute concentrations to adsorbent sites is lower, which cause an increase in dye removal. As shown in Fig. 6 (a, c, d) at higher dyes concentrations, lower adsorption yield is due to the saturation of adsorption sites. On the other hand, the dyes removal percentage was higher at lower initial dye concentrations and smaller at higher initial concentrations, which clearly indicate that the adsorption of MG and SO from aqueous solution was dependent on their initial concentrations.

Fig. 6 (b, c) presents the interaction of pH with other variables. The increased removal percentage of MG was observed with an increased in pH. This is probable due to the fact that at low initial pH, as a result of protonation of the functional groups, the MWCNTs surface get positively charged and the strong repulsive forces between the cationic dyes molecules and adsorbent surface lead to significant decrease in the dye removal percentage. The increase in the initial pH lead to deprotonation of the active adsorption sites on the MWCNTs surface via electrostatic interaction and/or hydrogen bonding adsorbs the MG and SO molecules.

Fig. 6 (a) also reveal the remarkable contribution of ultrasound for increase in mass transfer that possible the rapid uptake and fast establishment of equilibrium. The initial high

adsorption rate is related to high available surface area and vacant site of adsorbent due to dispersion of adsorbent in to solution by ultrasonic power. It was found that more than 80% of MG removal was occurred in the first 3.0 min.

For the adsorbent dosage, the response surfaces plots shown in Fig 6(b, d) demonstrated the changes in response as a function of adsorbent dosage and other variables with interaction of them. The percentage removal increased with an increase in adsorbent dosage due to its high specific surface area and small particle size. At higher value probably due to increase in surface area and availability of more active adsorption sites the rate of adsorption significantly increased. At lower amount of adsorbent, the removal percentage because of high ratio of dye molecule to vacant site significantly decreased.

3.4. Optimization of CCD by DF for extraction procedure

The profile for predicted values and desirability option in the STATISTICA 7.0 software is used for the optimization process (Fig. 7). Profiling the desirability of responses involves specifying the DF for each dependent variable (removal percentage) by assigning predicted values. The scale in the range of 0.0 (undesirable) to 1.0 (very desirable) is used to obtain a global function (D) that should be maximized according to efficient selection and optimization of designed variables. The CCD design matrix results (Table 2) show the maximum (99.2%) and minimum (20.37) adsorption of MG, respectively. According to these values, DF settings for each dependent variable of removal percentage are depicted on the right hand side of Fig. 7: desirability of 1.0 was assigned for maximum removal (99.2%), 0.0 for minimum (20.37 %) and 0.5 for middle (59.78%). On the left hand side of Fig. 7 (bottom) show the individual desirability scores are illustrated, to calculate the removal percentage. Since desirability 1.0 was selected as the target value, the overall response obtained from these plots with the current level of each

variable in the model is depicted at the top (left) of Fig. 7. A view glance to figures shows that variable affect simultaneously the response and its desirability. On the basis of these calculations and desirability score of 1.0, maximum recovery (99.3 %) was obtained at optimum conditions set as: 6.0 min of sonication time, 0.022 g of adsorbent, initial MG concentration of 15 mg L^{-1} and initial SO concentration of 15 mg L^{-1} at pH 5.5. The validity of duplicate assenting experiments at the optimized value of all parameters was investigated. The results are closely co-related with the data obtained from desirability optimization analysis using CCD.

3.5. Comparison with other methods

It may be seen from the table 4 that the contact time for proposed method in comparison with all of the adsorbents are preferable and superior and shows satisfactory removal performance for MG and SO.[6, 45, 46] The results indicated that the ultrasound assisted removal method has a remarkable ability to improve the removal efficiency of dyes. The ultrasonic-assisted enhancement of removal could be attributed to the high-pressure shock waves and high-speed microjets during the violent collapse of cavitation bubbles. [47, 48]

In such procedure real applicability was investigated by spiking real samples including tap water and distilled water and it was found that more than 95% of dyes removal was achieved for all the dyes.

4. Conclusion

In this study, Cu-NWs-AC adsorbent was synthesized and characterized. Adsorbent was utilized to remove MG and SO dyes from aqueous medium in presence of ultrasound. The analysis of the results by CCD allows for the achievement of the following optimization point: 0.022 g of adsorbent, 6 min of contact time and 15 mg L^{-1} MG and 15 mg L^{-1} SO at a pH of 5.5.

It was found that application of ultrasound leads to significant enhancement in extent of adsorption and removal percentage of MG and SO from aqueous solutions. Combination of ultrasound with Cu-NWs-AC increased the dye removal percentage (more than 99%) by using small amount of adsorbent (0.022 g) in short time (6.0 min). This procedure may also be applicable for simultaneous removal of dyes from actual waste water. It was found that a small amount of adsorbent (0.022 g) can remove a large amount of MG (34 mg g^{-1}) and SO (34 mg g^{-1}). Finally, the proposed method has good potential in the removal of dyes from wastewater compared to several other adsorbents. The dada and methodology presented in this paper might be useful for designing the adsorbent for the treatment of actual effluent. Furthermore, strength of this study regards the possibility of use ultrasound devise as worldwide equipment.

Acknowledgement

The authors express their appreciation to the Graduate School and Research Council of the University of Yasouj for financial support of this work.

References

1. S.-T. Yang, S. Chen, Y. Chang, A. Cao, Y. Liu and H. Wang, *J. Colloid Interface Sci.*, 2011, **359**, 24-29.

2. F. P. de Sá, B. N. Cunha and L. M. Nunes, *Chem. Eng. J.*, 2013, **215**, 122-127.

3. T. Gan, J. Sun, S. Cao, F. Gao, Y .Zhang and Y. Yang, *Electrochim. Acta*, 2012, **74**, 151-157.

4. M. Roosta, M. Ghaedi, N. Shokri, A. Daneshfar, R. Sahraei and A. Asghari, *Spectrochim. Acta, Part A,* 2014, **118**, 55-65.

5. M. A. Ahmad and R. Alrozi, *Chem. Eng. J.*, 2011, **171**, 510-516.

6. M. Ghaedi, S. Haghdoust, S. N. Kokhdan, A. Mihandoost, R. Sahraie and A. Daneshfar, *Spectro. Lett.*, 2012, **45**, 500-510.

7. M. Roosta, M. Ghaedi, A. Daneshfar and R. Sahraei, *Spectrochim. Acta, Part A,* 2014, **122**, 223-231.

8. M. Ghaedi, H. Khajehsharifi, A. H. Yadkuri, M. Roosta and A. Asghari, *Toxicol. Environ. Chem.*, 2012, **94**, 873-883.

9. G. Dotto and L. Pinto, *J. Hazard. Mater.*, 2011, **187**, 164-170.

10. M. Ghaedi, K. Mortazavi, M. Jamshidi, M. Roosta and B. Karami, *Toxicol. Environ. Chem.*, 2012, **94**, 846-859.

11. M. Ghaedi, H. Khajesharifi, A. Hemmati Yadkuri, M. Roosta, R. Sahraei and A. Daneshfar, *Spectrochim. Acta, Part A,* 2012, **86**, 62-68.

12. M. Ghaedi, D. Elhamifar, M. Roosta and R. Moshkelgosha, *J. Ind. Eng. Chem.*, 2014, **20**, 1703-1712.

13. M. Ghaedi, K. Niknam, S. Zamani, H. Abasi Larki, M .Roosta and M. Soylak, *Mater. Sci. Eng.: C*, 2013, **33**, 3180-3189.

14. M. Shamsipur, H. R. Rajabi, S. M. Pourmortazavi and M. Roushani, *Spectrochim. Acta, Part A,* 2014, **117**, 24-33.

15. M. Ghaedi, A .Ghaedi, F. Abdi, M. Roosta, A. Vafaei and A. Asghari, *Ecotoxicol. Environ. Saf.*, 2013, **96**, 110-117.

16. H. Treviño-Cordero, L. Juárez-Aguilar, D. Mendoza-Castillo, V. Hernández-Montoya, A. Bonilla-Petriciolet and M. Montes-Morán, *Ind. Crops Products*, 2013, **42**, 315-323.

17. M. Ghaedi, Z. Rozkhoosh, A. Asfaram, B. Mirtamizdoust, Z. Mahmoudi and A. A. Bazrafshan, *Spectrochim. Acta, Part A,* 2015, **138**, 176-186.

18. J. P. d. S. Fernandes, B. S. Carvalho, C. V. Luchez, M. J. Politi and C. A. Brandt, *Ultrason. Sonochem.*, 2011, **18**, 489-493.

19. O. Hamdaoui and E. Naffrechoux, *Ultrason. Sonochem.*, 2009, **16**, 15-22.

20.A. N. Chermahini, A. Teimouri, F. Momenbeik, A. Zarei, Z. Dalirnasab, A .Ghaedi and M. Roosta, *J. Hetero. Chem.*, 2010, **47**, 913-922.

21. S. Sonawane, P. Chaudhari, S. Ghodke, M. Parande, V. Bhandari, S. Mishra and R. Kulkarni, *Ultrason. Sonochem.*, 2009, **16**, 351-355.

22. Y. Li, A. S. Fabiano-Tixier, V. Tomao, G. Cravotto and F. Chemat, *Ultrason. Sonochem.*, 2013, **20**, 12-18.

23. M. Roosta, M. Ghaedi, A. Daneshfar, R. Sahraei and A. Asghari, *Ultrason. Sonochem.*, 2014, **21**, 242-252.

24. M. Roosta, M. Ghaedi, A. Daneshfar, S. Darafarin, R. Sahraei and M. Purkait, *Ultrason. Sonochem.*, 2014, **21**, 1441-1450.

25. M. Geng and S. M. Thagard, *Ultrason. Sonochem.*, 2013, **20**, 618-625.

26. D. Markovic, Z. Saponjic, M. Radoicic, T. Radetic, V. Vodnik, B. Potkonjak and M. Radetic, *Ultrason. Sonochem.*, 2015, **24**, 221-229.

27. P. Saharan, G. R. Chaudhary, S. Lata, S. Mehta and S. Mor, *Ultrason. Sonochem.*, 2015, **22**, 317-325.

28. O. Moumeni and O. Hamdaoui, *Ultrason. Sonochem.*, 2012, **19**, 404-409.

29. M. Hauptmann, F. Frederickx, H. Struyf, P. Mertens, M. Heyns, S. De Gendt, C. Glorieux and S. Brems, *Ultrason. Sonochem.*, 2013, **20**, 69-76.

30. S. Chakma and V. S. Moholkar, *Chem. Eng. J.*, 2011, **175**, 356-367.

31. G. L. Maddikeri, A. B. Pandit and P. R. Gogate, *Ind. Eng. Chem. Res.*, 2012, **51**, 6869-6876.

32. İ. Küncek and S. Şener, *Ultrason. Sonochem.*, 2010, **17**, 250-257.

33. F. Momenbeik, M. Roosta and A. A. Nikoukar, *J. Chromatogr. A*, 2010, **1217**, 3770-3773.

34. M. Roosta, M. Ghaedi and A. Daneshfar, *Food Chem.*, 2014, **161**, 120-126.

35. M. Chaichi, A. Mohammadi and M. Hashemi, *Microchem. J.*, 2013, **108**, 46-52.

36. M. Ghaedi, E. Shojaeipour, A. M. Ghaedi and R. Sahraei, *Spectrochim. Acta, Part A,* 2015, **142**, 135-149.

37. P. F. Martins, C. Carmona, E. L. Martinez, P. Sbaite, R. M. Filho and M. R. W. Maciel, *Sep. Pur. Technol.*, 2012, **98**, 464-471.

38. M. B. Hossain, N. P. Brunton, A. Patras, B. Tiwari, C. O'Donnell, A .B. Martin-Diana and C. Barry-Ryan, *Ultrason. Sonochem.*,, 2012, **19**, 582-590.

39. G. Derringer, *J. Qual. Technol.*, 1980, **12**, 214-219.

40. Q. Darugar, W. Qian, M. A. El-Sayed and M.-P. Pileni, *The J. Phys. Chem. B*, 2006, **110** , 143-149.

41. M. Roosta, M. Ghaedi, A. Daneshfar, R. Sahraei and A. Asghari, *J. Ind. Eng. Chem.*, 2015, **21**, 459-469.

42. Y. Chang, M. L. Lye and H. C. Zeng, *Langmuir*, 2005, **21**, 3746-3748.

43. J. Zhao, D. Zhang and X. Zhang, *Surf. Interface Anal.*, 2015, **47**, 529-534.

44. R. Sahraei, G. M. Aval and A. Goudarzi, *J. Alloys Compound.*, 2008, **466**, 488-492.

45. T. Santhi, S. Manonmani and T. Smitha, *J. Hazard. Mater.*, 2010, **179**, 178-186.

46. H. Zhang, Y .Tang, X. Liu, Z. Ke, X. Su, D. Cai, X. Wang, Y. Liu, Q. Huang and Z. Yu, *Desalination*, 2011, **274**, 97-104.

47. S. Shirsath, D. Pinjari, P. Gogate, S. Sonawane and A. Pandit, *Ultrason. Sonochem.*, 2013, **20**, 277-286.

48. P. R. Gogate, V. S. Sutkar and A. B. Pandit, *Chem. Eng. J.*, 2011, **166**, 1066-1082.

Figure captions:

Fig. 1. (a) Chemical structures of malachite green and (b) safranin O.

Fig. 2. (a) UV-Vis absorption spectrum of the Cu nanowires and (b) X-ray diffraction (XRD) pattern of the Cu nanowires loaded on activated carbon.

Fig. 3. FESEM images of (a) the activated carbon and (b) the Cu nanowires loaded deposited on activated carbon.

Fig. 4. (**a**) EDS mapping and (**b**) EDS analysis of the Cu-NWs-AC adsorbent.

Fig. 5. (A, B) The experimental data versus the predicted data of normalized removal of MG.

Fig. 6. Response surfaces for the CCD: MG concentration–Sonication time; (b) Adsorbent dosage–pH; (c) SO concentration–pH and (d) MG concentration–Adsorbent dosage.

Fig. 7. Profiles for predicated values and desirability function for removal percentage of MG. Dashed line indicated current values after optimization.

Table 1. Experimental factors and levels in the central composite design

Factors	Levels			Star point α=2.0	
	Low (−1)	Central (0)	High (+1)	−α	+α
(X_1) Sonication time (min)	2.0	3.5	5.0	0.5	6.5
(X_2) pH	3.0	5.0	7.0	1.0	9.0
(X_3) Adsorbent dosage (g)	0.009	0.015	0.021	0.003	0.027
(X_4) MG concentration (mg L^{-1})	10	15	20	5	25
(X_5) SO concentration (mg L^{-1})	10	15	20	5	25

Table 2. Experimental conditions and values obtained through the CCD

Runs	X_1	X_2	X_3	X_4	X_5	MG Removal (%)	SO Removal (%)
1	2	3	0.009	10	20	22.11	24.24
2	2	3	0.009	20	10	20.37	24.24
3	2	3	0.021	10	10	85.53	89.29
4	2	3	0.021	20	20	46.51	61.28
5	2	7	0.009	10	10	57.16	31.548
6	2	7	0.009	20	20	47.12	21.188
7	2	7	0.021	10	20	74.87	59.43
8	2	7	0.021	20	10	55.40	44.17
9	5	3	0.009	10	10	50.75	53.39
10	5	3	0.009	20	20	36.97	39.51
11	5	3	0.021	10	20	91.11	90.42
12	5	3	0.021	20	10	91.75	91.70
13	5	7	0.009	10	20	76.15	52.80
14	5	7	0.009	20	10	79.84	58.47
15	5	7	0.021	10	10	99.20	97.93
16	5	7	0.021	20	20	86.30	74.86
17 (C)	3.5	5	0.015	15	15	66.68	61.98
18 (C)	3.5	5	0.015	15	15	77.23	72.51
19 (C)	3.5	5	0.015	15	15	67.97	63.77
20	0.5	5	0.015	15	15	43.60	41.84
21	6.5	5	0.015	15	15	83.68	74.23
22	3.5	1	0.015	15	15	48.16	78.50
23	3.5	9	0.015	15	15	72.31	56.62
24	3.5	5	0.003	15	15	21.92	16.91
25	3.5	5	0.027	15	15	90.19	90.00
26	3.5	5	0.015	5	15	84.55	78.48
27	3.5	5	0.015	25	15	63.39	59.46
28	3.5	5	0.015	15	5	87.40	84.74
29	3.5	5	0.015	15	25	61.59	55.28
30 (C)	3.5	5	0.015	15	15	72.12	66.51
31 (C)	3.5	5	0.015	15	15	74.72	67.98
32 (C)	3.5	5	0.015	15	15	72.49	68.48

Table 3. Analysis of variance (ANOVA) for CCD

Source of variation	Sum of square	Degree of freedom	Mean square	F- value	P- value
X_1	3340.95	1	3340.953	209.9830	0.000028
X_1^2	131.13	1	131.126	8.2415	0.034962
X_2	1338.46	1	1338.461	84.1239	0.000258
X_2^2	257.94	1	257.936	16.2116	0.010057
X_3	5914.91	1	5914.912	371.7594	0.000007
X_3^2	471.73	1	471.732	29.6489	0.002837
X_4	758.55	1	758.551	47.6759	0.000976
X_4^2	6.43	1	6.430	0.4042	0.552902
X_5	508.48	1	508.479	31.9585	0.002406
X_5^2	10.58	1	10.584	0.6652	0.451803
X_1X_2	7.40	1	7.399	0.4650	0.525584
X_1X_3	5.17	1	5.171	0.3250	0.593292
X_1X_4	143.49	1	143.487	9.0183	0.029994
X_1X_5	0.62	1	0.621	0.0390	0.851159
X_2X_3	1043.42	1	1043.417	65.5800	0.000465
X_2X_4	14.36	1	14.360	0.9026	0.385725
X_2X_5	123.96	1	123.961	7.7911	0.038388
X_3X_4	149.26	1	149.257	9.3810	0.028011
X_3X_5	3.35	1	3.347	0.2103	0.665746
X_4X_5	0.27	1	0.268	0.0169	0.901725
Lack of Fit	127.93	6	21.322	1.3401	0.382742
Pure Error	79.55	5	15.911		
Total SS	14389.07	31			

Adsorbent	Adsorbate	Concentration (mg L^{-1})	Contact time (min)	Ref
Ricinus communis	MG	50	90	[45]
Brown-rotted pine wood	MG	7	600	[46]
Activated carbon	SO	25	80	[6]
MWCNT	SO	25	26	[6]
$Cd(OH)_2$-NW-AC	SO	25	23	[6]
Cu-NWs-AC	MG	15	6.0	Proposed method
Cu-NWs-AC	SO	15	6.0	Proposed method

Table 4. Comparison for the removal of dyes by different methods and adsorbents

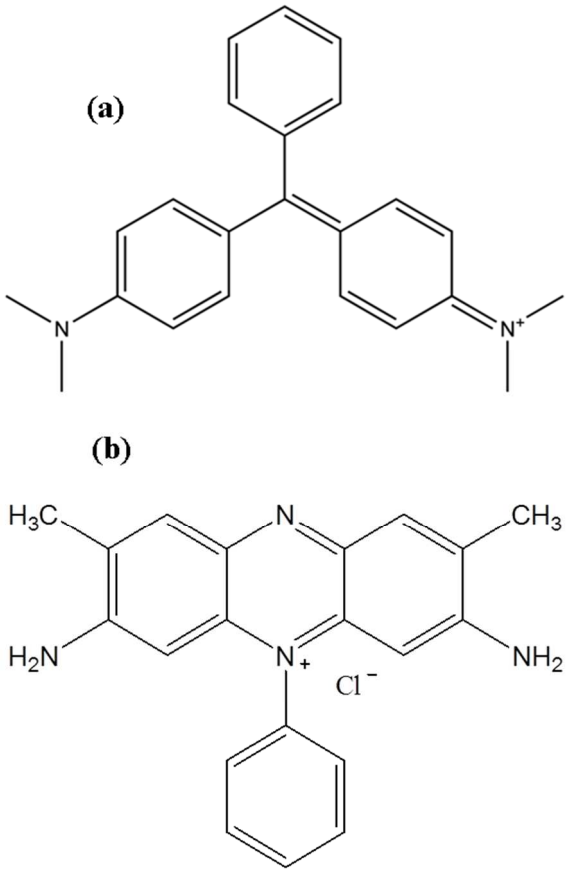

Fig. 1.

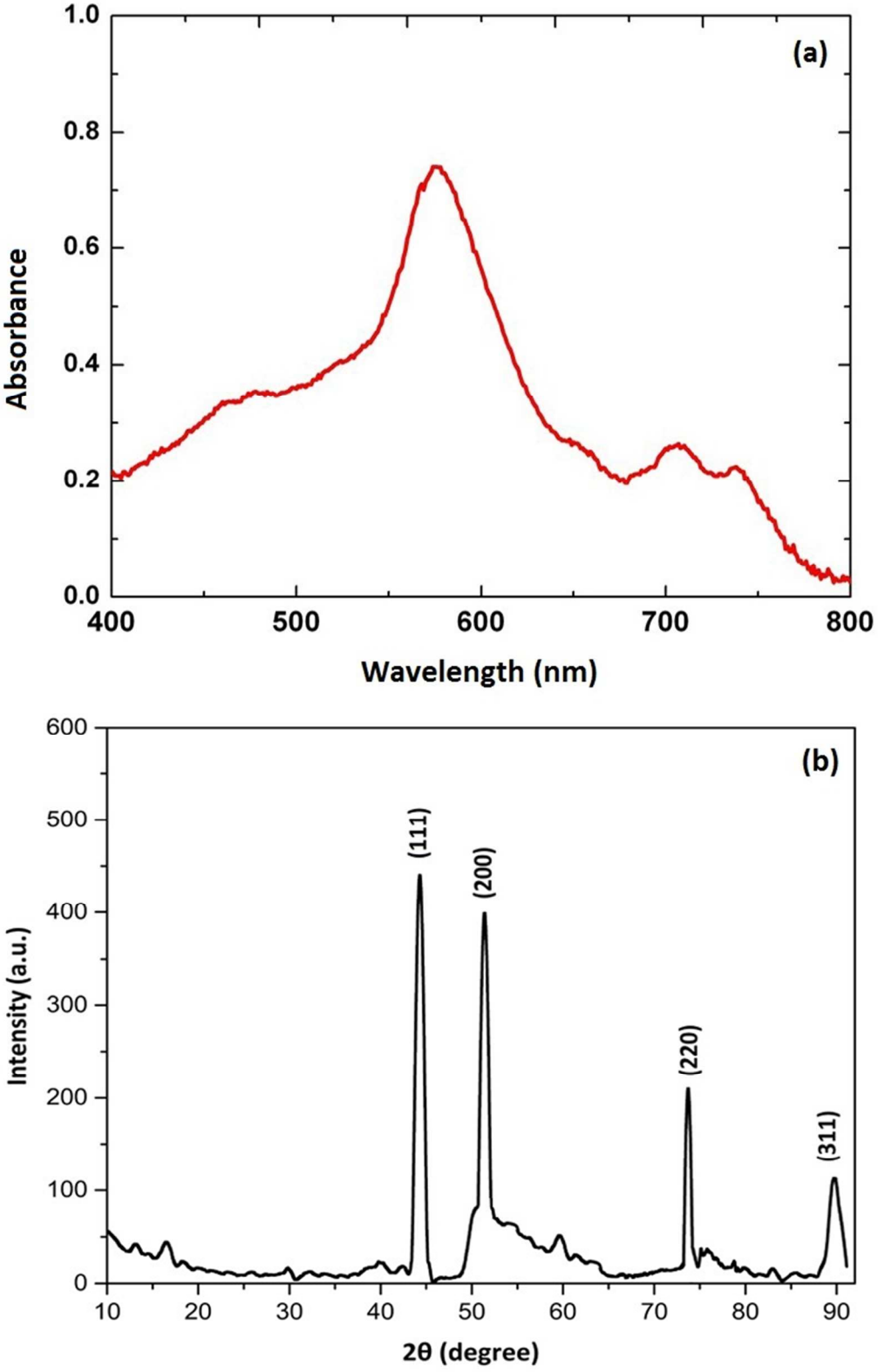

Fig. 2.

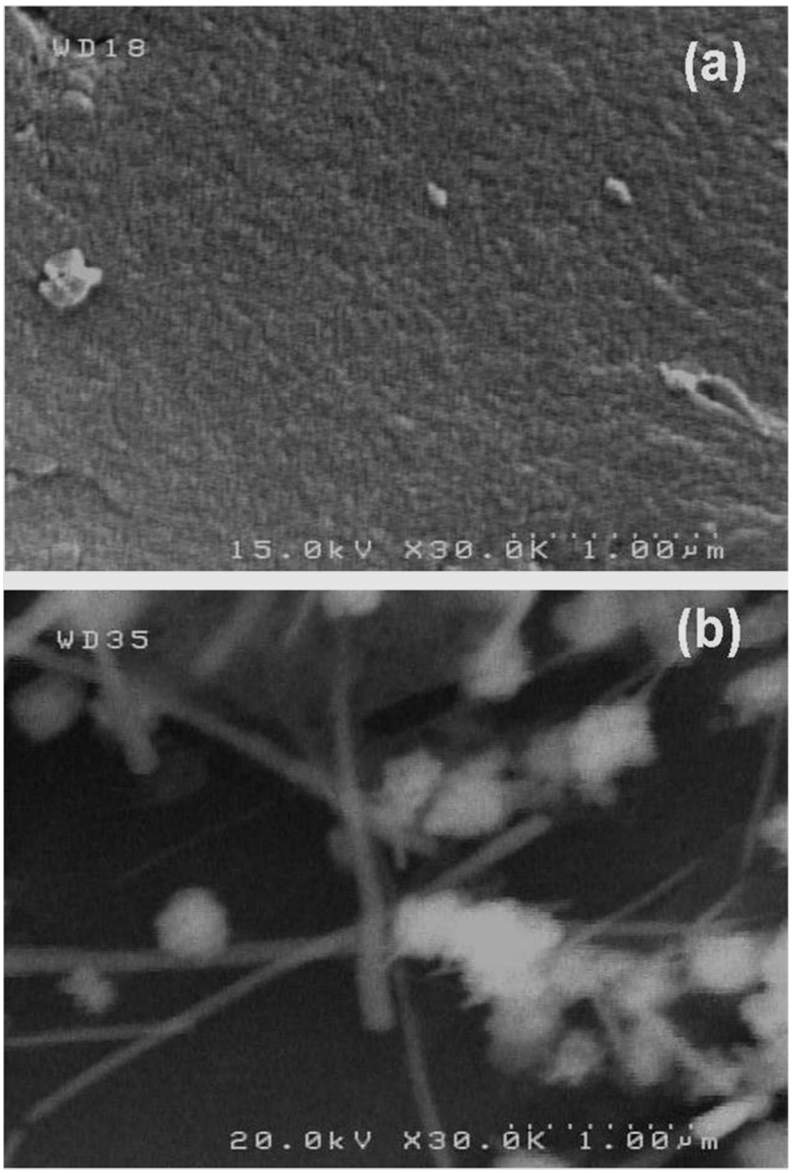

Fig. 3.

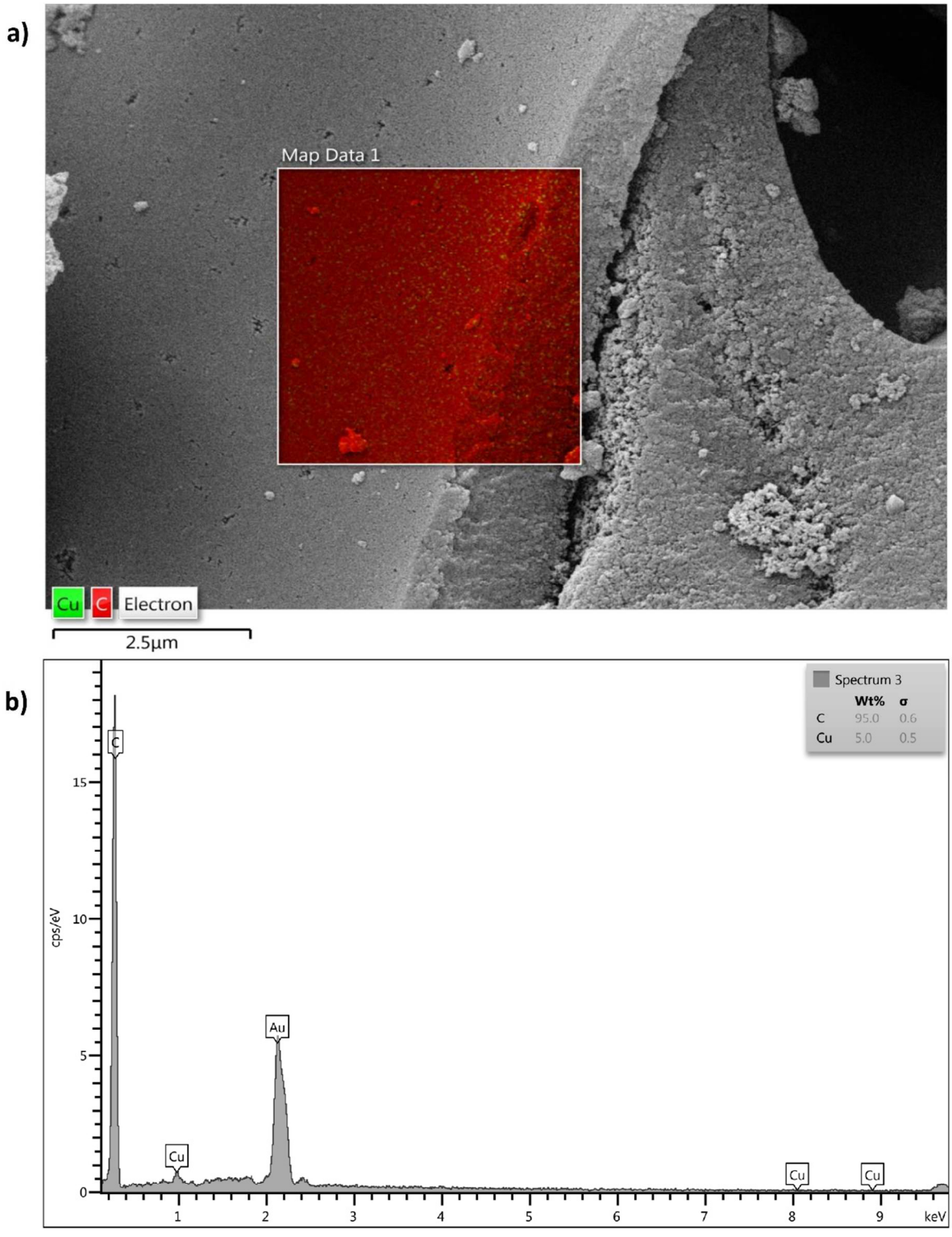

Fig. 4.

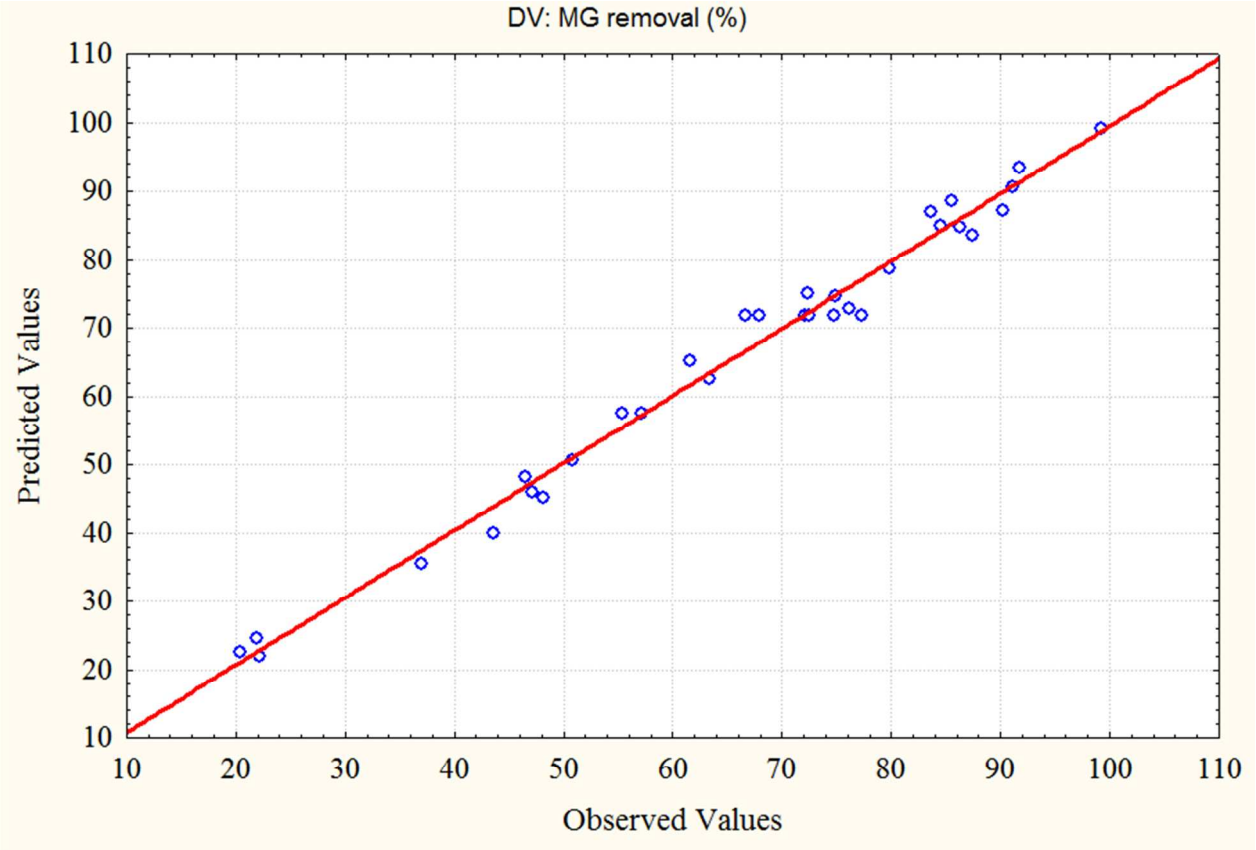

Fig. 5.

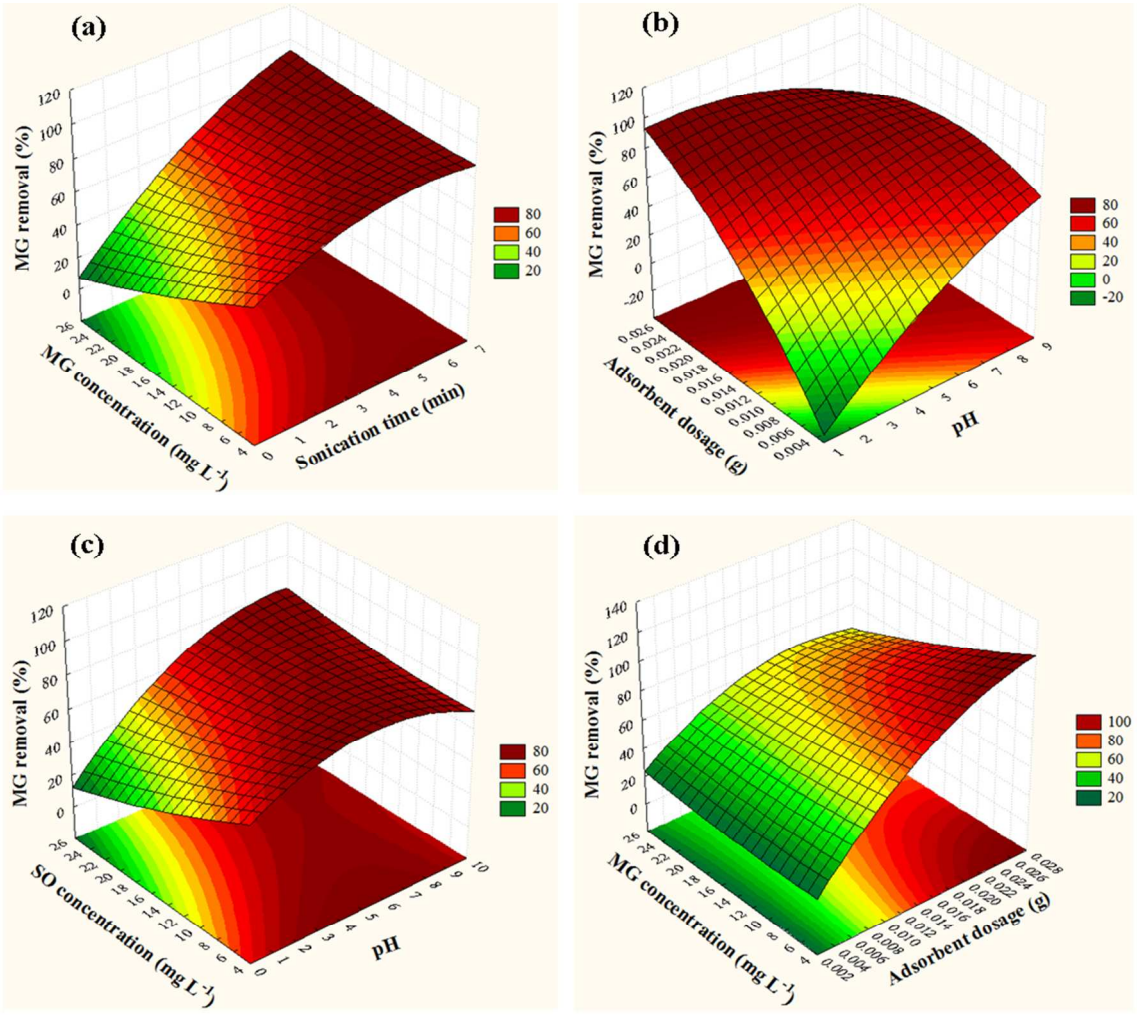

Fig. 6.

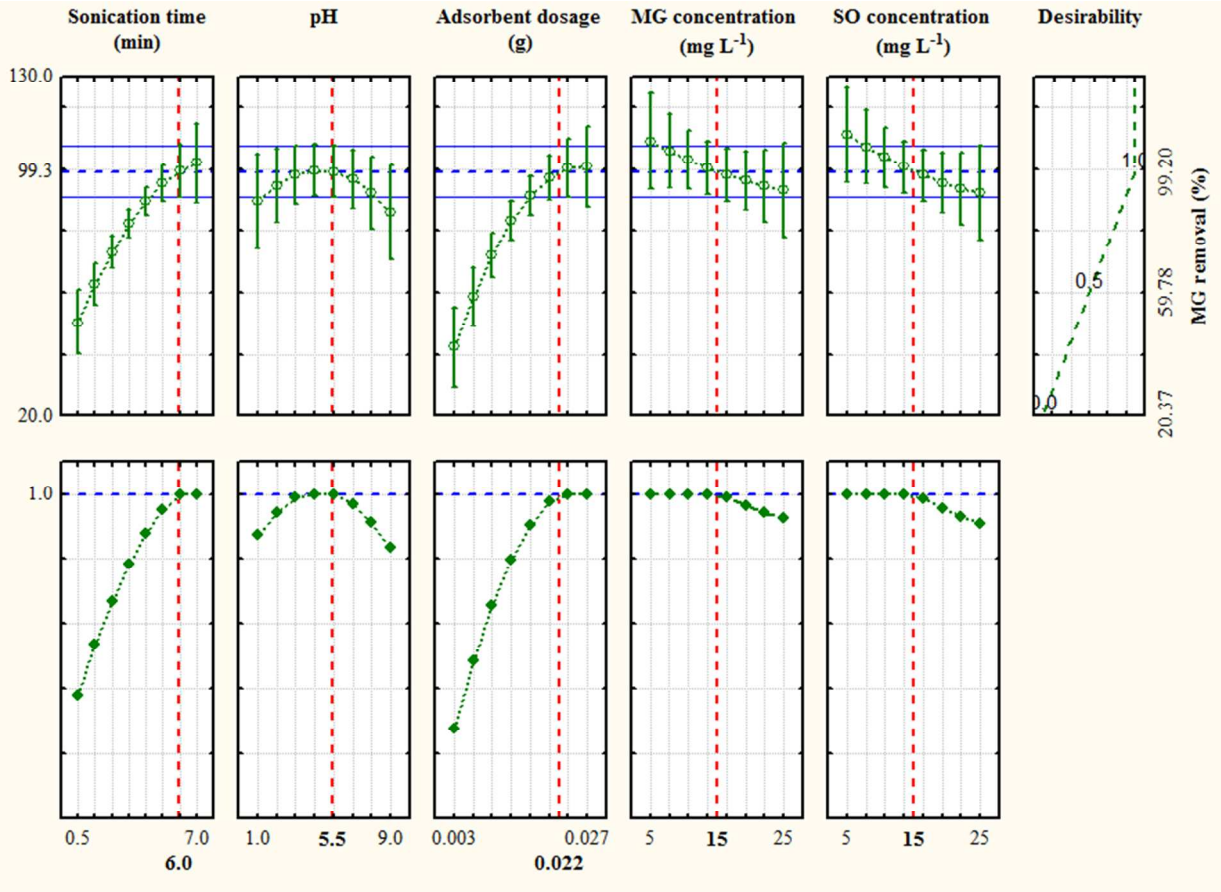

Fig. 7.